Author's Accepted Manuscript

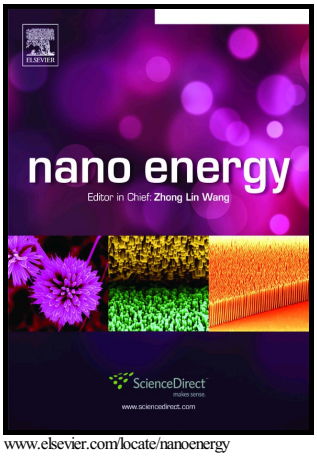

www.elsevier.com/locate/nanoenergy

Self-powered Hybrid Flexible Nanogenerator and its application in Bionic Micro Aerial Vehicles

Guowu Wei, Yaqi Bi, Xiuhan Li, Dongdong Xu, Wei Xu, Lung-Jieh Yang, Yong Qin, Haiyang Guo, Xuejun Zhao, Xiangyu Chen, Limin Jia

PII: S2211-2855(18)30694-3
DOI: https://doi.org/10.1016/j.nanoen.2018.09.050
Reference: NANOEN3055

To appear in: *Nano Energy*

Received date: 28 August 2018
Accepted date: 20 September 2018

Cite this article as: Guowu Wei, Yaqi Bi, Xiuhan Li, Dongdong Xu, Wei Xu, Lung-Jieh Yang, Yong Qin, Haiyang Guo, Xuejun Zhao, Xiangyu Chen and Limin Jia, Self-powered Hybrid Flexible Nanogenerator and its application in Bionic Micro Aerial Vehicles, *Nano Energy,* https://doi.org/10.1016/j.nanoen.2018.09.050

Self-powered Hybrid Flexible Nanogenerator and its application in Bionic Micro Aerial Vehicles

Guowu Wei [a1], Yaqi Bi [a1], Xiuhan Li [a*], Dongdong Xu [a], Wei Xu [a], Lung-Jieh Yang [b], Yong Qin [c*], Haiyang Guo [a], Xuejun Zhao [c], Xiangyu Chen[d], Limin Jia [c]

[a]School of Electronics and Information Engineering, Beijing Jiaotong University, Beijing 100044, PR China

[b]Mechanical and Electromechanical Enigneering, Tamkang University, Tamsui 25137, Taiwan

[c]State Key Laboratory of Rail Traffic Control and Safety, Beijing Jiaotong University, Beijing 100044, PR China

[d]Beijing Institute of Nanoenergy and Nanosystems, Chinese Academy of Sciences, Beijing 100083, PR China

[*]Corresponding author:Xiuhan Li and Yong Qin

Abstract

With the successive advent of piezoelectric nanogenerator (PENG) and triboelectric nanogenerator (TENG), the harvest of ambient mechanical energy has become more high-efficient, low-lost and simpler for self-powered systems. Introducing lightweight alternative power source to bionic micro aerial vehicle (BMAV) which is widely used for military surveillance or monitoring air pollution and so on, is the forefront of the research hotspots. However, there is still no design applying the two kinds of nanogenerator (NG) together in BMAV to collect the flapping mechanical energy more efficiently. In this paper, we demonstrate a hybrid flexible nanogenerator (HFNG) based on the combination of triboelectric and piezoelectric devices in BMAV. It not only can solve the problem of power supply, but also make the BMAV intelligent to monitor the changes of specific environmental factors. The newly designed HFNG can produce a maximum open-circuit voltage of 80 V, short-circuit current of 3.0 μA with the instantaneous output power density of 34.1 mW/m^2 when the flapping frequency of BMAV (*f*) is 14 Hz. The rectified output of HFNG has been applied to charge the commercial capacitor, rechargeable battery and drive light-emitting diodes. It was also demonstrated that HFNG can be used for testing the lift force (*L*) of BMAV. Moreover, the output performances of HFNG have been proved to be sensitive to temperature, humidity, alcohol concentration and PM2.5 in the environment.

Graphical abstract:

[1] Guowu Wei and Yaqi Bi contributed equally to this work

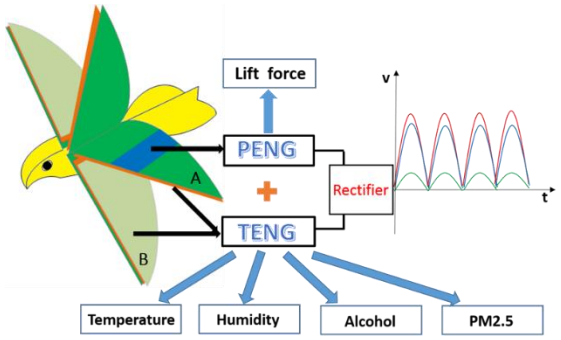

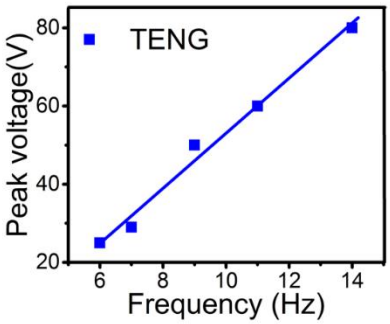

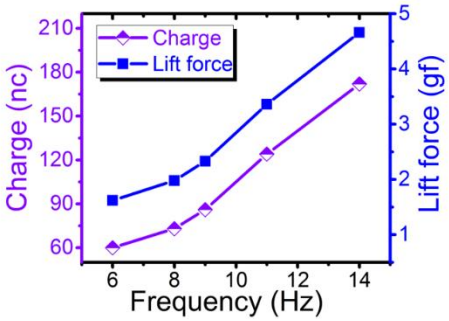

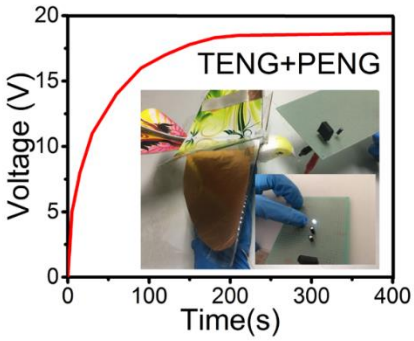

With the successive advent of piezoelectric nanogenerator (PENG) and triboelectric nanogenerator (TENG), the harvest of ambient mechanical energy has become more high-efficient, low-lost and simpler for self-powered systems. Introducing lightweight alternative power source to bionic micro aerial vehicle (BMAV) which is widely used for military surveillance or monitoring air pollution and so on, is the forefront of the research hotspots. However, there is still no design applying the two kinds of nanogenerator (NG) together in BMAV to collect the flapping mechanical energy more efficiently. In this paper, we demonstrate a hybrid flexible nanogenerator (HFNG) based on the combination of triboelectric and piezoelectric devices in BMAV. It not only can solve the problem of power supply, but also make the BMAV intelligent to monitor the changes of specific environmental factors. The newly designed HFNG can produce a maximum open-circuit voltage of 80 V, short-circuit current of 3.0 μA with the instantaneous output power density of 34.1 mW/m^2 when the flapping frequency of BMAV (f) is 14 Hz. The rectified output of HFNG has been applied to charge the commercial capacitor, rechargeable battery and drive light-emitting diodes. It was also demonstrated that HFNG can be used for testing the lift force (L) of BMAV. Moreover, the output performances of HFNG have been proved to be sensitive to temperature, humidity, alcohol concentration and PM2.5 in the environment.

Keyword:
piezoelectric nanogenerator, triboelectric nanogenerator, bionic micro aerial vehicle, hybrid, flexible, intelligent

1. Introduction

Nanogenerator has become a new technology to harvest mechanical energy and as a source of power for self-driving sensors, which provides the advantages of low cost, easy fabrication, light

weight, high efficiency and a wide choice of materials [1]. The piezoelectric nanogenerator (PENG), based on the coupling of piezoelectric and semiconducting properties of ZnO [2], was firstly proposed in 2007. The PENG makes it possible for nanodevices to harvest the mechanical energy in the environment and convert them into electrical energy for self-powering purpose. Its energy conversion efficiency is about 17~30%. Comparing with PENG, the triboelectric nanogenerator (TENG), which was invented in 2012 to harvest ambient environmental energy effectively [3], based on the coupling mechanism of triboelectric effect and electrostatic effect, shows a higher energy conversion efficiency of about 50-80%. In addition, the amazing characteristics, availability, efficiency and stability [4], keep surprising researchers with the continuous development of TENG. TENG has four basic working modes: vertical contact-separation mode [5-7], single electrode mode [8], lateral sliding mode [9] and independent layer mode [10]. The vertical contact-separation mode is particularly well adapted for transforming mechanical vibration and clapping energy into electrical energy. Several applications in the actual scene, like acoustic energy harvesting, wind energy harvesting and human body movement induced mechanical energy collecting, have been proposed by Yang et al.[11], Bae et al.[12] and Pu et al.[13]. To improve the efficiency of energy collection and maximize the use of resources, we propose a hybrid flexible nanogenerator (HFNG) in this paper by using these two kinds of nanogenerators synchronously. The HFNG obviously will have a higher energy harvesting efficiency than TENG because of the extra PENG contribution.

In the 1990s, the Defense Advanced Research Projects Agency (DARPA) firstly proposed the concept of the bionic micro aerial vehicle (BMAV) [14]. BMAV is characterized by small size, high aerial mobility, minimal materials, and low cost [15]. Typical envisioned tasks for BMAVs involve search, surveillance or monitoring of air pollution [16]. There are three basic kinds of BMAV based on the actuation mode: fixed-wing, flapping-wing, and rotary-wing BMAV. Compared with fixed-wing BMAV and rotary-wing BMAV, flapping-wing BMAV has the advantage of light weight because the flapping-wing does not need additional power equipment, like propeller or ducted fan, and provides a natural convenience in the bionic design [17-19]. However, one major unsolved problem in BMAV performance is the tardy progress in lightweight power source design. A well-designed BMAV can only weigh dozens of grams, however, over half of the weight was occupied by the battery. Therefore, introducing alternative power source to BMAV is the forefront of the research hotspots. So, in this paper, we ingeniously apply the HFNG in flapping-wing BMAV because of its high energy harvesting efficiency, light weight and flexibility. And we also demonstrated that the HFNG applied in BMAV not only can be used for a power supply of microelectronic devices, but also is potential to act as a sensor to monitor the specific environmental factors.

2. Structure and Theory

Figure 1a shows the holistic structure of HFNG applied in the flapping-wing BMAV. The HFNG is mainly composed of two parts, TENG and PENG. And we can also see that these two parts are physically isolated by the upper wing of BMAV. In addition to being able to harvest the mechanical energy of wings flapping to generate electricity, the two parts individually can accomplish different function. The PENG can be used to test the lift force of BMAV, and the TENG can monitor the changes of some environmental factors, such as temperature, humidity, alcohol concentration, PM2.5 and so on under certain conditions. Because of its high tensile

strength, wear resistance, impact toughness and chemical inertness, FEP (Fluorinated ethylene propylene) with thickness of 25 μm is selected as the body material of the BMAV wings. The manufacturing process of the TENG component can be summarized as: Firstly, nano copper layers was sputtered separately by PVD as the contact electrode and the back electrode on the inner surface of the two upper and lower symmetrical wings. Then a PTFE (Polytetrafluoroethylene) layer functions as the triboelectric material, is tightly attached on the copper layer at the lower wing. And the thickness of PTFE is around 0.01 mm. The surface of PTFE film is modified with etching nanostructures in order to increase the effective contact area (Figure 1b). Figure 1c shows the cross sections of wing A and wing B and the working process of TENG component. The PENG component is composed of a PVDF (Polyvinylidene fluoride) layer with thickness of 52 μm, and the both sides of PVDF film are sputtered with a silver electrode layer. Finally, the PVDF layer is attached to the outer surface of the upper wing of BMAV. In general, HFNG can generate a higher output than TENG and PENG.

The biggest advantage for HFNG is to be perfectly embedded in the flapping-wing BMAV. HFNG can effectively harvest the mechanical energy of wings flapping and convert it to electrical energy. And HFNG has a very slight impact on the flight of the BMAV itself due to flexibility and lightness of materials. Especially, the BMAV becomes intelligent because of sensitive output performances of HFNG under different circumstances. Moreover, we also provide a method to test the lift force of BMAV by HFNG. The overall quality of BMAV is probably 20 g and the BMAV without HFNG only weighs about 19.5 g. So, the HFNG applied in BMAV has a very broad application prospect for wireless sensor network node, military surveillance or environmental monitoring and so on.

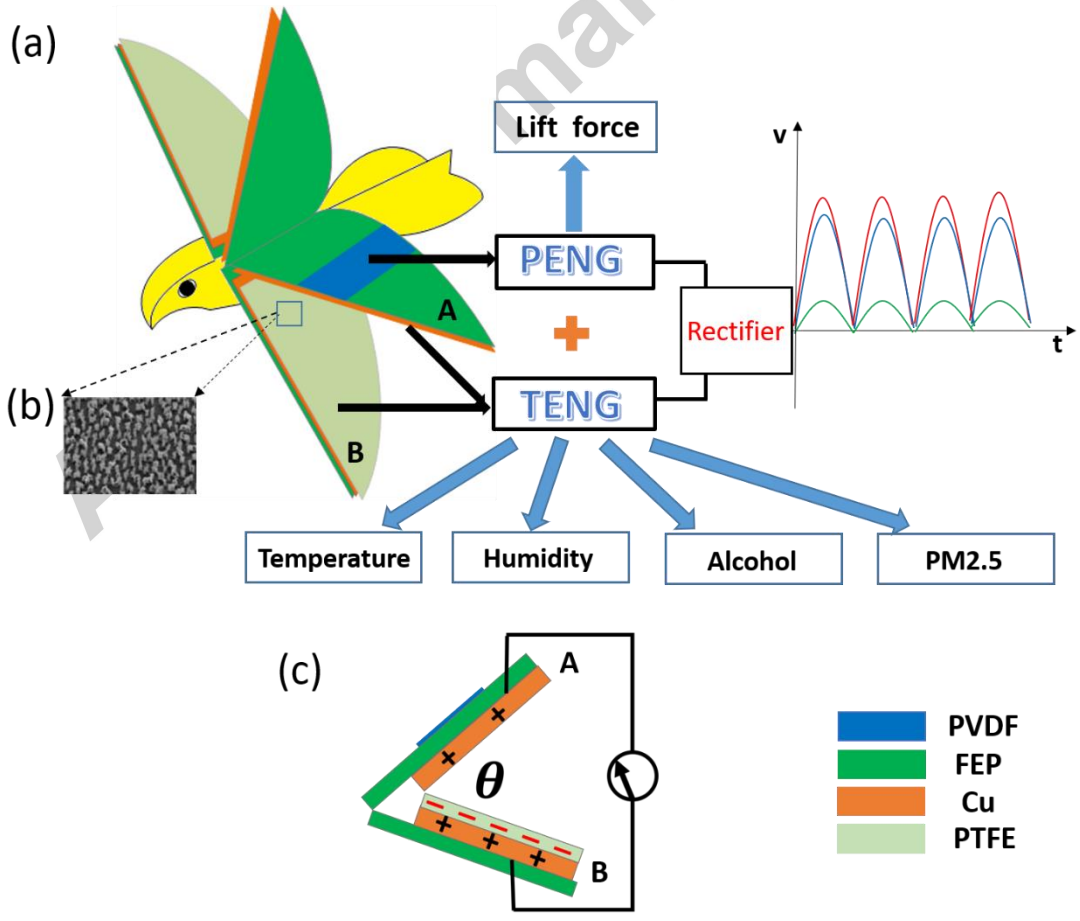

Figure 1 (a): The schematic diagram of the whole structure of HFNG applied in the BMAV and the functions of each component. (b): SEM image of the etching nanostructures on the PTFE surface. (c): The equivalent cross section diagram of wing A and wing B.

The working principle of TENG component is based on the mixing of vertical contact-separation mode. The cycle of the charge generation process is depicted in Figure 2a. Due to the coupling effect of electrification and electrostatic induction [5], the periodic contact and separation between two materials with opposite triboelectric polarities induce a current in the external circuit. At the initial state, the two wings are separated from each other. When starting the flapping-wing BMAV, the external force drives the two wings to contact each other. According to the triboelectric sequence [20-22], the electrons on the copper surface will transfer to the PTFE surface, so that the PTFE surface is negatively charged, and the copper surface is positively charged. When the two wings are separated at a certain angle, a potential difference will form between the two electrodes. Therefore, the induced electrons will flow through the external circuit from the lower electrode to the upper electrode. When the angle between the two wings reaches the maximum, the positive triboelectric charges on the contact electrode are almost completely neutralized by the induced electrons. After that, the external force drives two wings gradually move back towards each other, the decreases of electric potential difference between the two electrodes will drive the flow of electrons in the external circuit in the opposite direction.

At the same moment, PENG is also working to generate a periodic current in an external circuit because PVDF film is deformed by stress. As shown in Figure 2b, the working mechanism of PENG can be simply described as: When the BMAV starts to work, PVDF film will deform by external mechanical stress, resulting in its internal charges polarization that positive and negative charges transfer to the two surfaces, respectively [23]. So, the electric potential difference is formed between the upper surface and lower surface of PVDF film, which will force the electrons to flow from an electrode to another electrode until reaching the equilibrium. When the compressive strain is gradually released, the accumulated electrons will flow back to the primary electrode. Therefore, it forms the reverse current by the external circuit.

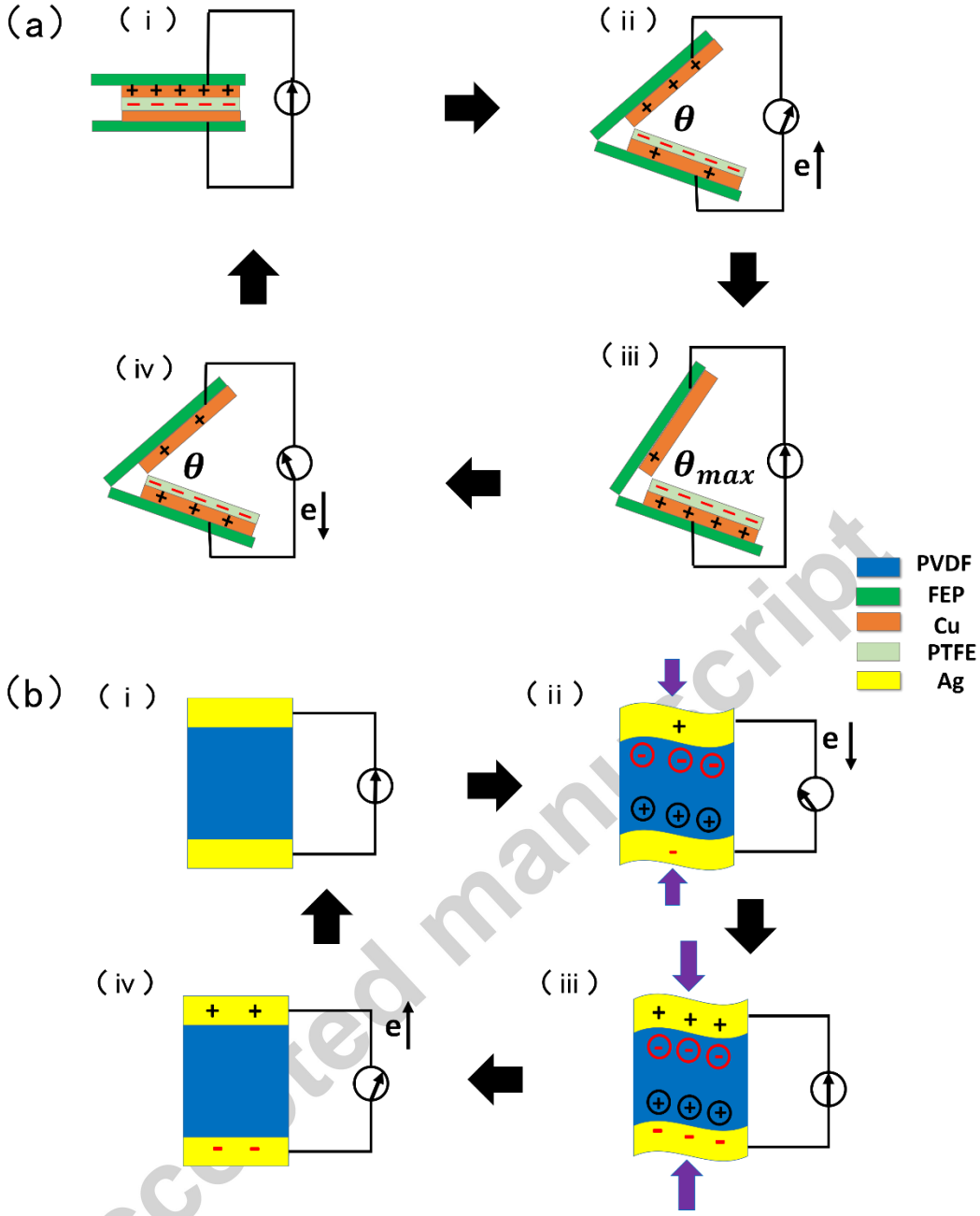

Figure 2 (a). The working principle of TENG component. (i) The external force drives the two wings contact each other, positive and negative triboelectric charges are generated on the copper surface and the PTFE surface, respectively. (ii) The external force drives the two wings separate at a certain angle, electric potential difference drives inducing electrons flow from back electrode to contact electrode. (iii) The included angle reaches the maximum, the positive triboelectric charges on the contact electrode are almost completely neutralized. (iv) Electrons are driven back from the contact electrode to the back electrode because the external force drives two wings gradually come closer to each other. (b) The working principle of PENG component. (i) PVDF film is in a state of rest. (ii) The internal charges of PVDF film polarize by external stress, forming the current through external circuit. (iii) The flow of electrons reaches an equilibrium state and the external current gradually reduces to zero. (iv) When the compressive strain is released, the electrons will flow in the opposite direction, which forms the reverse external current.

3. Results and Discussion

To characterize output performances of the HFNG, the open-circuit voltage (V_{oc}) and short-circuit (I_{sc}) were measured for PENG and TENG respectively at certain flapping frequency of BMAV, as shown as Figure 3. The surface area of used PVDF film is about 15.4 cm^2, which can produce a maximum open-circuit voltage of 3.2 V (Figure 3a) and a short-circuit current of 2.8 nA (Figure 3b) when the flapping frequency (f) is 14 Hz. The effective contact area of TENG is about 50 cm^2, which can produce a maximum open-circuit voltage of 80V and a short-circuit current of 3.0 μA at f = 14 Hz. It is worth pointing out that in order to improve the output performances of TENG, the surface of PTFE film has been applied with a strong electric field for minutes to increase charge density before measuring. Compared with PENG, TENG produces a higher output. So TENG is taken as the main energy harvesting component and PENG can be used for monitoring the changes of lift force of BMAV, which will be verified in the later sections. We can also observe that the number of peaks in one second is exactly the flapping frequency of BMAV according to Figure 3, which further verifies the periodic output characteristics of TENG and PENG.

To demonstrate the impact of the flapping frequency of BMAV on HFNG output performances, we separately tested the output peak voltage and current of PENG and TENG by changing the flapping frequency. These results are shown in Figure 4. According to the Figure 4, we can conclude that the output peak voltage and current are all positively related with the flapping frequency whether it is for PENG or TENG. It can be explained that the faster the wings flap, the more severe the PVDF deforms, and a larger quantity of charges is polarized in the inner of PVDF film, resulting in improving the outputs of PENG [24-25]. In addition, the deformation is larger near the closer to the tip of the wings, but the surface area of PVDF film will be limited. So PVDF film was attached near the middle region of the wing for a comprehensive consideration, as shown as Figure 1a. For the TENG, the relative velocity of the contact or separation of two wings and contact strength will be increased when enhancing the flapping frequency, which turns out producing a higher output voltage and current [26].

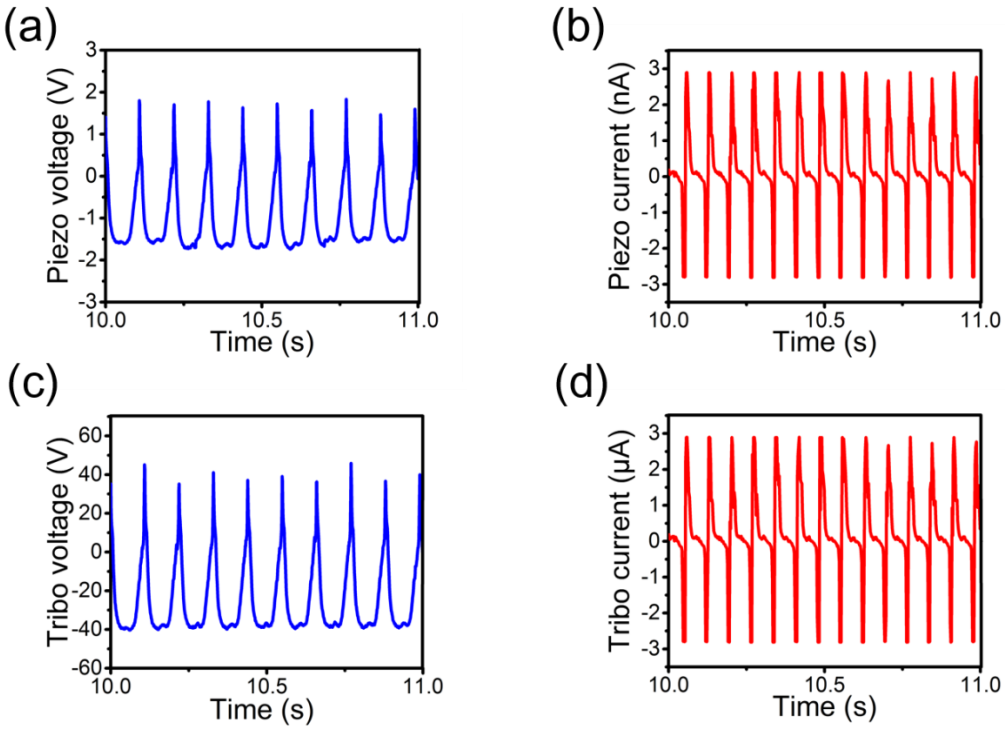

Figure 3. The measurement results of open-circuit voltage (a and c) and short-circuit current (b and d) at f = 14 Hz for PENG and TENG respectively.

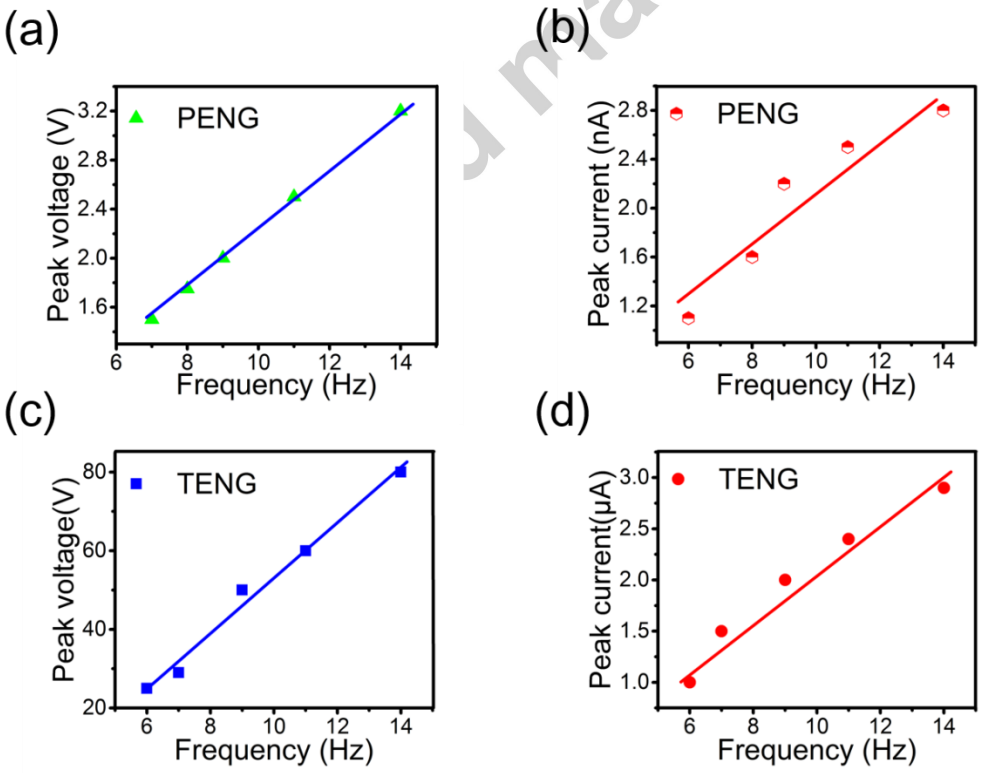

Figure 4. The characteristic curves of output peak voltage and current with different flapping frequency. The output peak voltage (a) and current (b) generated by PENG. The output peak

voltage (c) and current (d) generated by TENG.

The most important function for PENG is to be used for measuring the lift force of flapping-wing BMAV in the paper. The lift force measurement can be described as following mathematical formula. We regard $\Delta p(x,y,z)$ as an average pressure distribution between the upper and the lower sides of the flapping wings. So, we can think approximately:

$$\Delta p(x,y,z) = \frac{L}{A} \tag{1}$$

Where L is the half-winged lift force, A is the half-winged area. At the same time, we assume the BMAV as a plane-stress problem ($\sigma_z = 0$). Therefore, the plane-stress distribution on the flapping wings can be represented by $\sigma_x(x,y,z)$ and $\sigma_y(x,y,z)$. The charge density $\rho_z(x,y,z)$ along the Z-direction can be derived as [27]:

$$\rho_z(x,y,z) = d_{31}\sigma_x(x,y,z) + d_{32}\sigma_y(x,y,z) \tag{2}$$

Where d_{31} and d_{32} are non-zero coefficient of PVDF film. d_{31} = 20pc/N, d_{32} = 2pc/N. Meanwhile, $\sigma_x(x,y,z)$ and $\sigma_y(x,y,z)$ can be derived as:

$$\sigma_i(x,y,z) = \Delta p(\frac{a}{h})^2\beta_i \qquad i = x,y \tag{3}$$

Where a is the width of PVDF film, h is the thickness of PVDF film. So, we can approximately get the total charge Q generated by PENG as follows:

$$Q = \rho_z(x,y,z) \times S \tag{4}$$

Where S is the surface area of PVDF film. So, we can get the value of lift force of BMAV by measuring the value of Q according to equation (1)-(4).

$$L = \frac{A \times Q}{S\left(\frac{a}{h}\right)^2 (d_{31} \times \beta_x + d_{32} \times \beta_y)} \tag{5}$$

According to equation (5), we can conclude that L is positively proportional to Q. In order to verify the relationship between the lift force (L) of flapping-wing BMAV and the amount of charges (Q) generated by PENG, we must first know that S only affects Q, and has no direct relationship with L. It's easy to know that the higher the flapping frequency is, the greater the lift force becomes. Therefore, we can infer that Q / S approaches a constant at a fixed flapping frequency. So, we have made a series of measurements for the charge Q by using different surface area PVDF film, as shown in Figure 5a (f = 9 Hz). According to the test results, it can also be concluded that Q is approximatively linear with S. Figure 5b shows the characteristic curves of charge (Q) and lift force (L) with different flapping frequency. In experiments, the thickness (h) of the PVDF film we used is 52 μm, the width (a) is 8.1 cm and the surface area (S) is 15.4 cm^2. The half-winged area (A) of BMAV is about 85 cm^2. As indicated in Figure 5b, the amplitude of Q gradually increases with the increase of flapping frequency. That is, L and Q maintain the same trend of change while the wings are flapping more quickly. So, we have made a correct conclusion about the relationship of L and Q. According to Figure 5b, we can also conclude that the Q generated by PENG is about 172 nc and L can approximately reach 4.7 gf at f = 14 Hz.

We have known that the electric outputs of TENG are far higher than the PENG according to the results of Figure 3 and Figure 4. So TENG is taken as the main energy harvesting component in this paper. To characterize the maximum output power density of TENG, different external load resistances are connected in parallel to the output. As indicated in Figure 5c, the voltage amplitude rises with increasing load resistance while the current follows a reverse trend. In particular, the

flapping frequency is consistent (about 10 Hz) in all different load resistance experiments. As displayed in Figure 5d, the instantaneous peak power reaches the maximum when the external load resistance is about 9.4 MΩ. So, we can conclude that the equivalent internal resistance of TENG is 9.4 MΩ. According to the conclusion, we can calculate that the maximum output power density is about 34.1 mW/m^2 (V^2/4RS, the effective contact area(S) of TENG is about 50 cm^2) when the flapping frequency (*f*) is 14 Hz. To improve output power density, it can be tuned from following aspects: (i) Ensuring the flatness and less air bubbles between materials in the process of manufacturing HFNG. (ii) Improving properly the flapping frequency of BMAV, but not too high, probably resulting in the body of BMAV shaking badly. (iii) Appropriately increasing effective contact area of TENG.

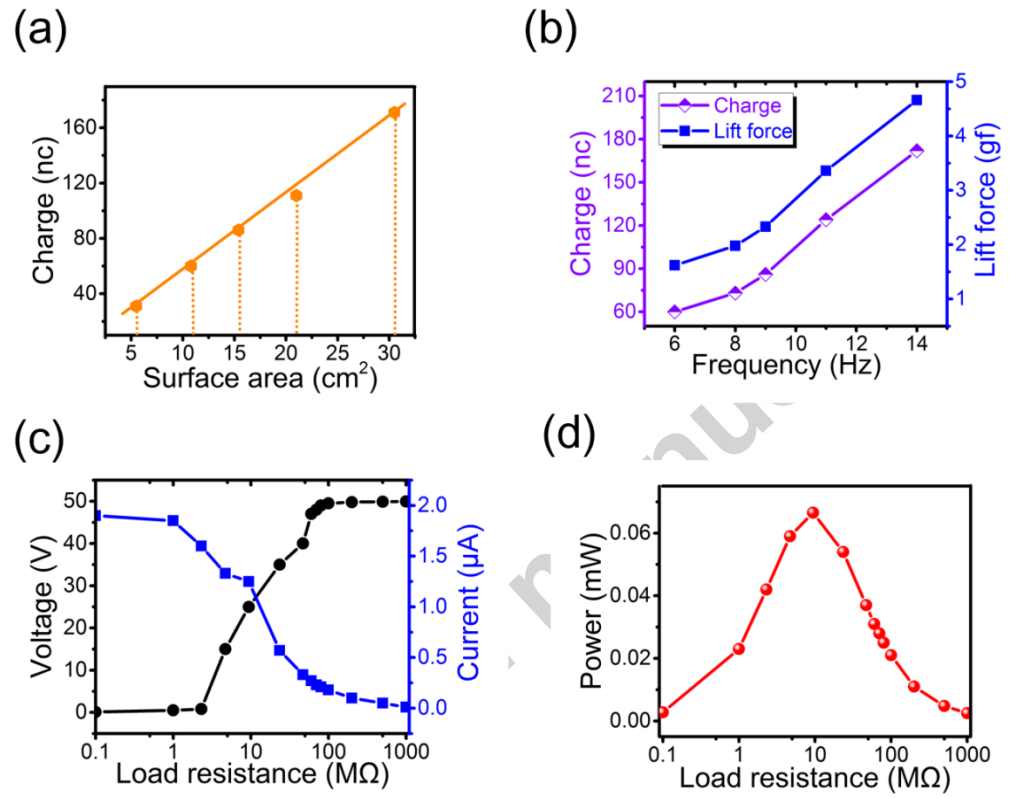

Figure 5. (a) The charge (*Q*) generated by PENG by using different surface area PVDF film. (b) The characteristic curves of charge (*Q*) and lift force (*L*) with different flapping frequency. (c) Output voltage and current of TENG in case of different external load resistance when the flapping frequency is 10 Hz. (d) Instantaneous output power characteristic curve with varying load resistance.

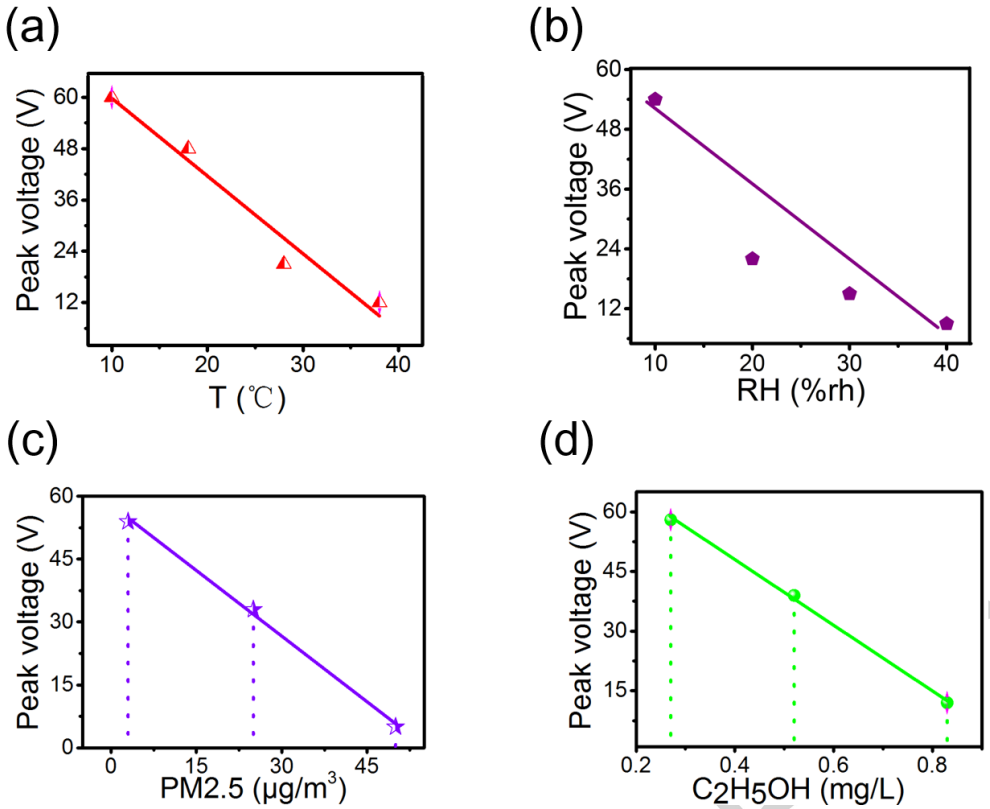

Figure 6: The output peak voltage (V_p) of TENG relative with some sensitive parameters when the flapping frequency is certain (about 11 Hz). (a) Peak voltage (V_p) varying with environmental temperatures (T). (b) The relationship between aerial relative humidity (RH) and V_p. (c) With the increase of PM2.5 concentration, the V_p is reduced. (d) The negative correlation between alcohol concentration (C_2H_5OH) and V_p.

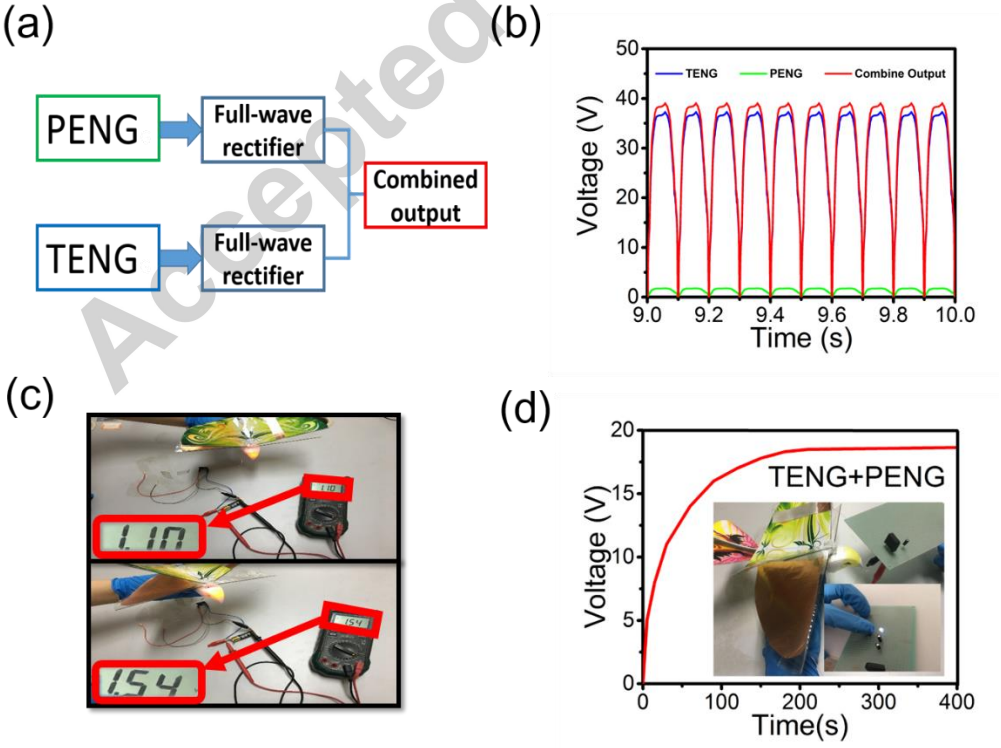

Figure 7. (a) The schematic block diagram of the combined output by PENG and TENG. (b) The output voltage generated by TENG and PENG with the full-wave rectifier and the combined output voltage. (c) The battery voltage before charging and after charging. (d) Charging curve of 4.7 pF capacitors and the demonstration of lighting commercial LED by HFNG.

To verify the output sensitive characteristics of TENG under different environmental conditions, four different kinds of measurements have been carried out by changing the specific environmental factor when the flapping frequency is certain (about 11 Hz). As shown in Figure 6a, the output peak voltage (V_p) of TENG is gradually reduced as the temperature rises, which is due to a change in the relative permittivity of PTFE film. The ability of storing and gaining electrons for PTFE becomes weakened, causing a decrease in the amount of charge on the inner surfaces of the wings [28]. The V_p of TENG is also a function of aerial relative humidity shown in Figure 6b. With the wings' periodic contact and separation, electrons transfer on two internal surfaces. As the humidity gradually increases, the surface of the material will adsorb water molecules, leading to a reduction of charge based on the triboelectric effect [29-30]. The relationship between PM2.5 concentration and V_p is shown in Figure 6c. PM2.5 is a particle with positive charge floating in the air. There is an electric field between two wings, which adsorbs these particles. Therefore, the charge density on the surface of the wings is reduced, leading to a lower V_p [31]. At the same time, we can also refer to *supporting video 1*. And Figure 6d shows the negative correlation between alcohol concentration and V_p. As alcohol molecules show negative polarity, the charge carrier accumulation layer near the surface of the wings will be thinned by attracting alcohol molecules. And that leads to less transferred charges, which account for a lower V_p [32-33]. As we can see, the output peak voltage (V_p) of TENG is negatively correlated with these four environmental factors. Of course, the real environment is complex. But if we can be sure that only one environmental factor among them changed a lot, the TENG is possible to be used for monitoring the changes of the environmental factor.

To demonstrate that HFNG can produce a higher output than TENG alone, the generated outputs by TENG and PENG were separately connected to a full-wave rectifying bridge to transform the AC outputs to a coincident direction. The simple schematic block diagram was shown in Figure 7a. The measurement results were shown in Figure 7b. According to the Figure 7b, we can see that most of the output voltages for HFNG is contributed by TENG. To prove the capability of HFNG as a sustainable power source, a rechargeable battery was charged by HFNG combining the energy harvesting power chip (LTC3588-1) (Figure S1). And the battery was charged from 1.10 V to 1.54 V after about 20 minutes' charging process, these results were shown in Figure 7c. Besides, a 4.7 pF capacitor was also charged by HFNG, and the charging curve was displayed in Figure 7d. As indicated in Figure 7d and *supporting video 2*, a commercial LED bulb was lighted up by HFNG with an energy processing circuit (Figure S2). So, the HFNG has the potential applications that charging for microelectronic devices or supplying for BMAV itself and so on. It is necessary to be added that these results shown in Figure 3, 4, 5 and 7 are all measured under a normal indoor environment. And the temperature and humidity are about 14 °C and 10% RH respectively while the concentration of alcohol and PM2.5 can be ignored.

4. Conclusions

In summary, we successfully developed a hybrid flexible nanogenerator (HFNG) applying

PENG and TENG together in flapping-wings BMAV. The HFNG can be efficient to harvest the flapping mechanical energy and convert it to electric energy because of the periodic contact and separation of the upper and lower wings. The newly designed HFNG produces a maximum open-circuit voltage of 80 V, short-circuit current of 3.0 μA with the instantaneous output power density of 34.1 mW/m^2 when the flapping frequency of BMAV (f) is 14 Hz. The electric output is related to effective contact area and the flapping frequency of BMAV. Besides, HFNG can be used for testing the lift force (L) of BMAV, and L is approximately 4.7 gf at f = 14 Hz. We also demonstrated that the output performances of HFNG applied in BMAV is sensitive to environmental temperature, humidity, PM2.5 and alcohol concentration, etc. The rechargeable battery has been charged successfully and the commercial LED was lighted after a free flight of BMAV for a period time, which indicates that HFNG is possible to be used for a power supply for microelectronic devices, wireless sensor network node or BMAV itself.

ACKNOWLEDGEMENT

This research is supported by the National Key Research and Development Program of China (No. 2016YFB1200203), National Natural Science Foundation of China (60706031 and 61574015), Beijing; National Science Foundation (4122058), Beijing Higher Education Young Elite Teacher Project (YETP0536), the State Key Laboratory of Rail Traffic Control and Safety (RCS2016K009), Beijing Jiaotong University and the "Talents Project" of Beijing Jiaotong University.

References

[1] X.X. Chen, Y. Song, Z.M. Su, H.T. Chen, X.L. Cheng, J.X. Zhang, M.D. Han, H.X. Zhang, Flexible fiber-based hybrid nanogenerator for biomechanical energy harvesting and physiological monitoring. Nano Energy, 2017, 38: 43–50.

[2] Z.L. Wang and J.H. Song Science, Piezoelectric Nanogenerators Based on Zinc Oxide Nanowire Arrays [J]. Science, 2006, 312(5771) April: 242-246.

[3] W.Q. Yang, J. Chen, G. Zhu, J. Yang, P. Bai, Y.J. Su, Q.S. Jing, X. Cao, and Z.L. Wang, Harvesting Energy from the Natural Vibration of Human Walking, ACS NANO, 2013.

[4] Wang Z L. Triboelectric nanogenerators as new energy technology for self-powered systems and as active mechanical and chemical sensors [J]. Acs Nano, 2013, 7(11):9533.

[5] Zhu G, Pan C F, Guo W X, Chen C Y, Zhou Y S, Yu R M, Wang Z L. Triboelectric-generator-driven pulse electrodeposition for micropatterning. Nano Lett, 2012, 12(9): 4960-4965.

[6] Wang S H, Lin L, Wang Z L. Nanoscale triboelectric-effect-enabled energy conversion for sustainably powering portable electronics. Nano Lett, 2012, 12(12): 6339-6346.

[7] Zhu G, Lin Z H, Jing Q S, Bai P, Pan C F, Yang Y, Zhou Y S, Wang Z L. Toward large-scale energy harvesting by a nanoparticle-enhanced triboelectric nanogenerator. Nano Lett, 2013, 13(2): 847-853.

[8] Yang Y, Zhou Y S, Zhang H L, Liu Y, Lee S M, Wang Z L. A single-electrode based triboelectric nanogenerator as self-powered tracking system. Adv Mater, 2013, 25(45): 6594-6601.

[9] Wang S H, Lin L, Xie Y N, Jing Q S, Niu S M, Wang Z L. Sliding-triboelectric nanogenerators based on in-plane charge-separation mechanism. Nano Lett, 2013, 13(5):

2226-2233.

[10] Wang S H, Xie Y N, Niu S M, Lin L, Wang Z L. Freestanding triboelectric-layer-based nanogenerators for harvesting energy from a moving object or human motion in contact and non-contact modes. Adv mater, 2014, 26(18): 2818-2824.

[11] Yang J, Chen J, Liu Y, et al. Triboelectrification-based organic film nanogenerator for acoustic energy harvesting and self-powered active acoustic sensing.[J]. Acs Nano, 2014, 8(3):2649-2657.

[12] Bae J, Lee J, Kim S M, et al. Flutter-driven triboelectrification for harvesting wind energy [J]. Nature Communications, 2014, 5:4929.

[13] Pu X, Li L, Song H, et al. A Self-charging Power Unit by Integration of a Textile Triboelectric Nanogenerator and a Flexible Lithium-Ion Battery for Wearable Electronics [J]. Advanced Materials, 2015, 27(15):2472.

[14] Steven Ashley. Palm-size spy plane [J]. Mechanical Engineering, 1998, 11 (3):74-78.

[15] Sawyer B. Fuller, Zhi Ern Teoh, Pakpong Chirarattananon, Néstor O. Pérez-Arancibia, Jack Greenberg, Robert J. Wood. Stabilizing Air Dampers for Hovering Aerial Robotics: Design, Insect-scale Flight Tests, and Scaling. Autonomous Robots, 2017:1-19.

[16] Gianluca Antonelli, Filippo Arrichiello, Stefano Chiaverini, Paolo Robuffo Giordano. Adaptive Trajectory Tracking for Quadrotor BMAVs in Presence of Parameter Uncertainties and External Disturbances. IEEE Transactions on Control Systems Technology, 2017, PP (99):1-7.

[17] Shkarayev S V, Ifju P G, Kellogg J C, et al. Introduction to the Design of Fixed-Wing Micro Air Vehicles Including Three Case Studies[J]. 2015.

[18] C.K. Hsu. The Preliminary Design, Fabrication, and Testing of Flapping Micro Arial Vehicles (Ph.D., Tamkang University, Taiwan 2008), p.116 (In Chinese).

[19] Shyy W, Aono H, Chimakurthi S K, et al. Recent progress in flapping wing aerodynamics and aeroelasticity[J]. Progress in Aerospace Sciences, 2010, 46(7):284-327.

[20] Henniker J. Triboelectricity in Polymers. Nature, 1962, 196 (4853): 474.

[21] McCarty L S, Whitesides G M. Electrostatic charging due to separation of ions at interfaces: Contact electrification of ionic electrets. Angew Chem Int Ed, 2008, 47 (12): 2188-2207.

[22] Lacks D J, Sankaran R M. Contact electrification of insulating materials. J Phys D: Appl Phys, 2011, 44 (45): 453001.

[23] Kaiwai H. The piezoelectricity of polyvinydene fluoride [J]. Journal of applied Physics, 1969, 8 (7): 975-976.

[24] Chu B, Salem DR. Flexoelectricity in several thermoplastic and thermosetting polymers. Appl Phys Lett 2012; 101(10):103905.

[25] Jiabin Feng, Shouhu Xuan, Li Ding, Xinglong Gong Magnetoactive elastomer/PVDF composite film based magnetically controllable actuator with real-time deformation feedback property. COMPOSITES PART A-APPLIED SCIENCE AND MANUFACTURING 2017.09.004.

[26] Paresh Vasandania, Bharat Gattu, Zhi-Hong Mao, Wenyan Jia, Mingui Sun. Using a synchronous switch to enhance output performance of triboelectric nanogenerators. Nano Energy 43(2018) 210-218.

[27] Lung-Jieh Yang, Cheng-Kuei Hsu, Jen-Yang Ho, Chao-Kang Feng. Flapping wings with PVDF sensors to modify the aerodynamic forces of a micro aerial vehicle. Sensors and

Actuators A 139 (2007) 95-103.

[28] Lu, CX; Han, CB; Gu, GQ; Chen, J; Yang, ZW; Jiang, T; He, C; Wang, ZL; Temperature Effect on Performance of Triboelectric Nanogenerator; Advanced Engineering Materials;2017.

[29] Chang, TH; Peng, YW; Chen, CH; Chang, TW; Wu, JM; Hwang, JC; Gan, JY; Lin, ZH; Protein-based contact electrification and its uses for mechanical energy harvesting and humidity detecting; Nano Energy; 2016.

[30] Nguyen, V; Yang, RS; Effect of Humidity and Pressure on the Triboelectric Nanogenerator; Nano Energy; 2013.

[31] Guang Qin Gu, Chang Bao Han, Cun Xin Lu, Chuan He, Tao Jiang, Zhen Liang Gao, Cong Ju Li, and Zhong Lin Wang; Triboelectric Nanogenerator Enhanced Nanofiber Air Filters for Efficient Particulate Matter Removal; ACS Nano; 2017, 11 (6) :6211-6217

[32] Wen, Z; Chen, J; Yeh, MH; Guo, HY; Li, ZL; Fan, X; Zhang, TJ; Zhu, LP; Wang, ZL; Blow-driven Triboelectric Nanogenerator as an Active Alcohol Breath Analyzer; Nano Energy; 2015.

[33] Zhen Wen, Liping Zhu, Weimin Mei, Liang Hu, Yaguang Li, Luwei Sun, Hui Cai, Zhizhen Ye; Rhombus-shaped Co3O4 nanorod arrays for high-performance gas sensor; Sensors & Actuators B: Chemical, 2013, 186 (9) :172-179.

Video 1 : the comparison of output voltage for TENG when the concentration of PM2.5 is 11ug/m^3 and 22ug/m^3 respectively

Video 2 : a commercial LED bulb was lighted up by HFNG with an energy processing circuit

Highlights

- The electrical output of self-powered HFNG shows good linearity with flapping frequency of BMAV.
- The self-powered HFNG is sensitive to different environmental factors, for example temperature, humidity, alcohol concentration and PM2.5, etc.
- HFNG can be used to test the lift force of BMAV.
- HFNG can produce a higher output than TENG alone.